Scripta Materialia 130 (2017) 264–268

Contents lists available at ScienceDirect

Scripta Materialia

journal homepage: www.elsevier.com/locate/scriptamat

# Improving the intergranular corrosion resistance of austenitic stainless steel by high density twinned structure

A.Y. Chen [a,*], W.F. Hu [a], D. Wang [a], Y.K. Zhu [a], P. Wang [a], J.H. Yang [a], X.Y. Wang [a,*], J.F. Gu [b], J. Lu [c]

[a] School of Material Science & Engineering, University of Shanghai for Science and Technology, Shanghai, 200093, China
[b] School of Materials Science and Engineering, Shanghai Jiao Tong University, Shanghai, 200030, China
[c] Department of Mechanical and Biomedical Engineering, City University of Hong Kong, Hong Kong, China

ARTICLE INFO

*Article history:*
Received 17 October 2016
Received in revised form 24 November 2016
Accepted 25 November 2016
Available online xxxx

*Keywords:*
Stainless steel
Intergranular corrosion
Twinned structure
Passivation

ABSTRACT

We investigated the effect of high density twins on the intergranular corrosion (IGC) of austenitic stainless steel after sensitization. The twinned samples, especially the one with a twin density over 86% area fraction, exhibited a remarkable IGC resistance, characterized by a higher corrosion potential, a broader passivation zone, and a lower corrosion rate. The chromium depletion was inhibited by the twin boundaries emitted at grain boundaries, while the passivation was enhanced by the chromium enrichment at nanotwins inside the coarse grains.


Austenitic stainless steels (SS) of type 304 and 316 L are widely used as a structural material due to the good mechanical properties and excellent corrosion resistance [1,2]. However, intergranular corrosion (IGC) is a serious problem for austenitic SS exposed to aggressive temperature of 450–850 °C [3]. The major reason of IGC is the so-called sensitization, i.e., chromium depletion at grain boundary (GB) due to the precipitation of chromium carbide [4]. Twin boundary (TB), as a special low-energy boundary, can not only significantly improve the strength and ductility of the face-centered cubic metals [5–8], but also effectively suppress carbide precipitation at the GBs [9–12]. Thus, grain boundary engineering (GBE) concept is proposed to improve the IGC by creating discontinuous low-energy segments free of chromium carbide through the incident TBs at the GBs [13–15]. Limited by the small quantity of twins prepared by the conventional methods [16,17], the kernel thought of GBE is to manipulate the distribution of the low-energy TBs emitted at GBs [18–21]. It is expected that the high density twins should totally evade the chromium depletion at GBs, but no evidence has yet been obtained. More importantly, with the occurrence of high density twins, especially those in much refined scale, the function of TBs located inside the coarse grains (CG) should also be taken into account. Because TB networks occupy a larger area fraction compared with the GBs and they also are active interfaces relative to the regular crystal structure. Nevertheless, the effects of these TBs on the corrosion performance are missing in the GBE design. In this work, we examined IGC performance of 304 SSs with different twin densities by using the potentiodynamic polarization and mass loss tests. The effects of TB networks on the chromium depletion at the GBs and chromium enrichment at the TBs are investigated.

The chemical compositions of AISI 304 SS are 0.04 C, 0.49 Si, 1.65 Mn, 7.8 Ni, 16.8 Cr, 0.37 Mo and the balance Fe (all in mass%). The high density twins in nanoscale and submicroscale were produced by surface mechanical attrition treatment (SMAT) at a high impacting frequency. The detailed high-speed SMAT experimental setup and procedures were presented in Ref. [22]. The SMATed 304 SS was sensitized at 650 °C for 2 h and furnace cooling. Two types of twinned specimens after sensitization were prepared by polishing 100 and 250 μm depth from the surface, referred to as TW-100 and TW-250, respectively. Potentiodynamic polarization behaviors of the as-received 304 SS, the sensitized 304 SS and the twinned 304 SS samples were tested in 3.5% NaCl solution at a scan rate of 0.2 mV $s^{-1}$ after immersing for 10 min. Electrochemical impedance spectroscopy (EIS) measurements were performed under 5 mV amplitude of sinusoidal potential signals with respect to the open-circuit potential over a frequency range from 100 kHz to 10 mHz. The mass lose tests were carried out in 65% (wt%) $HNO_3$ solution at boiling temperature.

The microstructure of the sensitized 304 SS, TW-100 and TW-250 samples are given in Fig. 1. The grain size of the sensitized 304 SS (Fig. 1a) is about 15 μm. Deep grooves are clearly observed along the GBs. The magnification shows that rod-shaped precipitates with a length approx. 300 nm and a width 50 nm are formed inside the grooves, as indicated by the arrows in Fig. 1b. The line distribution of Fe, Cr, and Ni elements across the GB (dotted line in Fig. 1b) are shown in the lower

* Corresponding authors.
*E-mail addresses:* aychen@usst.edu.cn (A.Y. Chen), xianyingwang@usst.edu.cn (X.Y. Wang).

http://dx.doi.org/10.1016/j.scriptamat.2016.11.032
1359-6462/

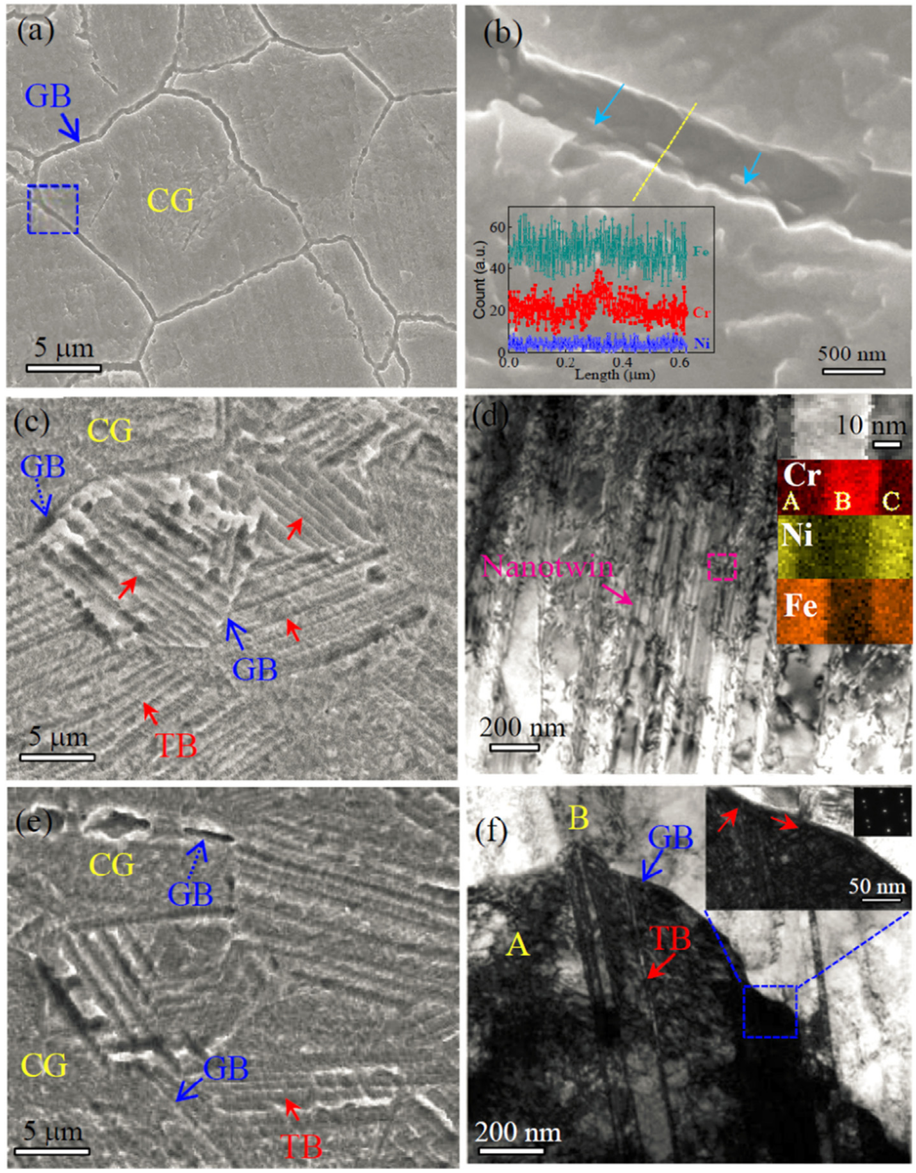


**Fig. 1.** The microstructure of the 304 SS and the twinned SS after sensitization at 650 °C for 2 h. (a) and (b) SEM images of the sensitized 304 SS; (c) and (d) are the SEM and TEM images of the TW-100 sample, respectively; (e) and (f) are the SEM and TEM images of the TW-250 sample, respectively; (b) is the magnification of the rectangular zone in (a) and the lower inset in (b) is the element distribution along the dotted line. The first upper inset in (d) is the magnification of the rectangular zone in (d), these lower insets are the mappings of Cr, Ni, and Fe elements from upper to lower. The upper inset in (f) is the SAED pattern of the grain A, and the relative lower inset is the magnification of the rectangular zone.

inset of Fig. 1b, where the rod-shaped precipitate exhibits a higher Cr content. The SEM images of TW-100 (Fig. 1c) and TW-250 (Fig. 1e) samples exhibit that most of the CGs contain high density twins with twin spacing in submicroscale and twin length in microscale, which separate the CGs into twin/matrix lamellar networks. The twin density is characterized by an area fraction of the grains containing twins to the total selected zone. The statistic data estimated from 10 pieces of SEM images show that the twin density is 86% for the TW-100 and 65% for the TW-250 specimens, respectively. Furthermore, the TEM image (Fig. 1d) of the TW-100 specimen displays that lots of nanotwins exist inside the grains. The insets in Fig. 1d are the mappings of the Cr, Ni, and Fe, elements in a nanotwin with a twin spacing of 30 nm, where the Cr atoms are enriched, and the Fe and Ni atoms correspondingly decrease. From the left to the right marked by A, B, and C in the second upper inset of Fig. 1d, the Cr content is 14.4%, 18.7%, and 14.0% (wt%), respectively. In order to observe the detailed interface structure of the GBs intersected with TBs, the TEM image of the TW-250 specimen is given in Fig. 1f. The GB between the two grains A and B is clear, no precipitation is observed along the whole GB. The grain A contains lots of nanotwins, which are emitted from the GB, as shown in the inset of Fig. 1f. The corresponding SAED pattern of grain A is given in the upper inset, which verifies the twinned structure.

Since the nanotwins are not stable thermally at higher temperature, therefore, the deformed nanotwins produced by the SMAT were used as the starting structure without further annealing at high temperature. The SEM and TEM observations both confirm that the high density nanotwins retain after sensitization at 650 °C (in Fig. 1c-f). The other research work found that the deformed nanotwins can endure the heat treatment up to 800 °C [23]. It should be mentioned that the deformed twins in the two twinned samples still contain high density dislocations after sensitization, as shown in Fig. 1d and f. Compared with the sensitized 304 SS, the two twinned samples have few grooves at the GBs with incident TBs. Nevertheless, a few GBs without incident TBs show deeper cracks, especially in the TW-250 sample, as indicated by dotted arrows in Fig. 1c and e. Moreover, no precipitation are observed in the SEM and TEM images of the twinned samples (Fig. 1c–f), indicating